British Journal of Pharmacology

British Journal of Pharmacology (2016) **173** 1805–1819 1805

RESEARCH PAPER

Preventive and chronic mineralocorticoid receptor antagonism is highly beneficial in obese SHHF rats

Correspondence Anne Pizard, Inserm U1116, CHRU Nancy, rue du Morvan, Vandoeuvre-lès-Nancy 54500 France. E-mail: anne.pizard@inserm.fr

Received 10 December 2015; **Revised** 17 February 2016; **Accepted** 23 February 2016

G Youcef[1,2,3,4], A Olivier[1,2,3,5], N Nicot[4], A Muller[4], C Deng[2,3,6], C Labat[1,2,3], R Fay[5,7], R-M Rodriguez-Guéant[2,3,5,8], C Leroy[1,7], F Jaisser[5,7], F Zannad[1,2,3,5,7], P Lacolley[1,2,3,5], L Vallar[4] and A Pizard[1,2,3,5,7]

[1]UMRS U1116 Inserm, Nancy, France, [2]Fédération de Recherche 3209, Nancy, France, [3]Université de Lorraine, Nancy, France, [4]Genomics Research Unit, Luxembourg Institute of Health, Luxembourg, [5]CHU Nancy, Nancy, France, [6]UMR 7365 CNRS, Nancy, France, [7]CIC 1433 Inserm, Pierre Drouin, Nancy, France, and [8]U954 Inserm, Nancy, France

BACKGROUND AND PURPOSE

Mineralocorticoid receptor (MR) activation contributes to heart failure (HF) progression. Its overactivity in obesity is thought to accelerate cardiac remodelling and HF development. Given that MR antagonists (MRA) are beneficial in chronic HF patients, we hypothesized that early MRA treatment may target obesity-related disorders and consequently delay the development of HF.

EXPERIMENTAL APPROACH

Twenty spontaneously hypertensive HF dyslipidaemic obese SHHF$^{cp/cp}$ rats and 18 non-dyslipidaemic lean SHHF$^{+/+}$ controls underwent regular monitoring for their metabolic and cardiovascular phenotypes with or without MRA treatment [eplerenone (eple), 100 mg · kg^{-1} · day^{-1}] from 1.5 to 12.5 months of age.

KEY RESULTS

Eleven months of eple treatment in obese rats (SHHF$^{cp/cp}$eple) reduced the obesity-related metabolic disorders observed in untreated SHHF$^{cp/cp}$ rats by reducing weight gain, triglycerides and total cholesterol levels and by preserving adiponectinaemia. The MRA treatment predominantly preserved diastolic and systolic functions in obese rats by alleviating the eccentric cardiac hypertrophy observed in untreated SHHF$^{cp/cp}$ animals and preserving ejection fraction (70 ± 1 vs. 59 ± 1%). The MRA also improved survival independently of these pressure effects.

CONCLUSION AND IMPLICATIONS

Early chronic eple treatment resulted in a delay in cardiac remodelling and HF onset in both SHHF$^{+/+}$ and SHHF$^{cp/cp}$ rats, whereas SHHF$^{cp/cp}$ rats further benefited from the MRA treatment through a reduction in their obesity and dyslipidaemia. These findings suggest that preventive MRA therapy may provide greater benefits in obese patients with additional risk factors of developing cardiovascular complications.

Abbreviations

aldo, aldosterone; BMI, body mass index; BNP, brain natriuretic peptide; ^{cp}, mutant ^{cp} allele of the leptin receptor; CSAA, cross-sectional adipocyte area; EDT, E wave deceleration time; EDV, end-diastolic volume; EF, ejection fraction; Einc, elastic incremental modulus; eple, eplerenone; ESV, end-systolic volume; Fn1, fibronectin 1; HDL, high-density lipoproteins; HF, heart failure; HW, heart weight; IR, insulin resistance; IVRT, isovolumetric relaxation time; LDL, low-density lipoproteins; Lepr, leptin receptor; LV, left ventricle; LVID, Left ventricle internal diameter; MR, mineralocorticoid receptor; MRA, mineralocorticoid receptor antagonist; Nox4, NADPH oxidase 4; PWT, posterior wall thickness; RAAS, renin–-angiotensin–aldosterone system; SHHF, spontaneously hypertensive heart failure; SWT, septum wall thickness; TG, triglycerides; TL, tibia length; VAT, visceral adipose tissue; Vim, vimentin

DOI:10.1111/bph.13479

Tables of Links

TARGETS
Nuclear hormone receptors[a]
Mineralocorticoid receptor (MR; NR3C2)
Catalytic receptors[b]
Leptin receptor

LIGANDS	
Adiponectin	Fibronectin
Aldosterone	Insulin
BNP	TGFβ2
COL3A1	TGFβ3
Corticosterone	

These Tables list key protein targets and ligands in this article which are hyperlinked to corresponding entries in http://www.guidetopharmacology.org, the common portal for data from the IUPHAR/BPS Guide to PHARMACOLOGY (Pawson *et al.*, 2014) and are permanently archived in the Concise Guide to PHARMACOLOGY 2015/16 ([a,b]Alexander *et al.*, 2015a,b).

Introduction

Over 23 million patients are diagnosed with heart failure (HF) worldwide (McMurray *et al.*, 1998) among whom 32 to 49% are obese (body mass index, BMI $\geq$ 30 kg·m^{-2}) and 31 to 40% are overweight (25 $\leq$ BMI $<$ 30 kg·m^{-2}) (Clark *et al.*, 2014). Obesity, along with the ageing of the population and the increased prevalence of various underlying pathophysiological mechanisms, also referred to as HF modifier conditions (van Deursen *et al.*, 2014), are known to precipitate individuals towards fully developed HF phenotypes.

Adverse adaptive mechanisms such as overactivation of the renin–angiotensin–aldosterone system (RAAS) are recognized to contribute to HF. Extensive study of the RAAS has resulted in the development of several pharmacological strategies aimed at inhibiting its unbalanced signalling pathways in HF. Accordingly, the addition of mineralocorticoid receptor (MR) antagonists (MRA) to standard treatments has been proven to alleviate HF symptoms and clearly reduce mortality in HF patients (Greenberg *et al.*, 2006; Iraqi *et al.*, 2009). Although initially believed to mainly regulate body fluid volumes via its interaction with the renal MR, extrarenal pathophysiological effects of its ligands, namely, aldosterone and corticosterone, have been substantiated by the finding that MRs are expressed in the myocardium of the failing heart and in non-epithelial target tissues such as adipose tissue (Caprio *et al.*, 2007; Zennaro *et al.*, 2009; Caprio *et al.*, 2011; Marzolla *et al.*, 2012. Excessive MR activation and increased aldosterone concentration have been implicated in the development of co-morbidities that are highly prevalent in HF patients. Whether alone (obesity, insulin resistance, diabetes and hypertension) or in combination (metabolic syndrome, MetS), they participate in a rapid deterioration of myocardial structure (remodelling) and function. Because increased aldosterone concentrations have also been reported in MetS, increased MR stimulation is thought to accelerate the pathophysiological conditions that lead to the development of HF (De Keulenaer and Brutsaert, 2011). Thus, when endeavouring to prevent or delay the development of HF, abnormal MR activity in non-cardiac co-morbidities appears as a potentially valuable target for new personalized therapeutic strategies. Although it is clear that obesity is an important risk factor for HF development, data remain relatively scarce regarding the contribution of MRAs in the prevention of the development of HF in obese patients. Given the proven role of MR activation in adipogenesis (Guo *et al.*, 2008; Feraco *et al.*, 2013), we hypothesized that early MRA treatment with eple, one of the most selective MRAs to date, may delay or attenuate the adverse cardiac remodelling and subsequently prevent HF progression especially in obese rats.

Our previous characterization of spontaneously hypertensive heart failure obese rats (SHHF$^{cp/cp}$, homozygous for the defective mutant ^{cp} allele of the leptin receptor gene Lepr) (Youcef *et al.*, 2014) demonstrated that the onset of metabolic disorders (dyslipidaemia, overweight and insulin resistance) as well as pre-hypertension occurred within the first 3 months of the life of these animals. These alterations appeared in the absence of any sign of cardiac dysfunction but nonetheless contributed to the earlier onset of HF in SHHF$^{cp/cp}$ rats as compared with their lean controls SHHF$^{+/+}$. Considering that SHHF$^{cp/cp}$ rats also develop an exacerbated hyperaldosteronism compared with SHHF$^{+/+}$ rats, the present study investigated whether early antagonism of the MR could sustainably improve the cardiovascular function of ageing SHHF rats and whether the effects of this treatment were modulated by the presence of metabolic alterations in SHHF$^{cp/cp}$ rats. To this end, SHHF rats were treated for 11 months (initiated at 1.5 months of age) with either the MRA eple as a mono-therapy or its placebo. Our conclusions with regard to the beneficial effects of chronic MRA are strengthened by the results observed with this treatment of both dyslipidaemic obese SHHF$^{cp/cp}$ rats and their non-dyslipidemic lean SHHF$^{+/+}$ controls.

Methods

Animal model

Animal studies are reported in compliance with the ARRIVE guidelines (Kilkenny *et al.*, 2010; McGrath and Lilley, 2015). One-month-old SHHF male rat littermates (SHHF/MccGmiCrl-Lepr^{cp}, Charles River Laboratories, USA) were genotyped (Ishizuka *et al.*, 1998) to determine their homozygocity for the wild-type '+' allele or the mutant 'cp' allele that encodes a defective leptin receptor, thus identifying the animals as the SHHF$^{+/+}$ or SHHF$^{cp/cp}$ genotype respectively. The experimental protocols were carried out in our laboratory after a 2-week acclimatization period within the animal care facility where rats were allowed *ad libitum* access

to fluid and food (Purina Formulab chow 5008, Charles River, USA). This protocol was designed according to the ARRIVE guidelines (http://onlinelibrary.wiley.com/doi/10.1111/j.1476-5381.2010.00872.x/pdf). It was approved by the 'Comité d'Éthique Lorrain en Matière d'Expérimentation Animale' (CELMEA) under agreement no. 0.1886 and was performed in an authorized animal facility (agreement no. C 54–547-17). This agreement defined appropriate end-points, which limited the amount of pain an animal suffered during the development of the HF phenotype; end points (survival study) were set as being lack of mobility of the animal and the development of congestion. Changes in the behaviour of the animals were assessed daily and supported by their regular phenotyping. Animals with the most noticeable phenotype were intensely monitored but none of them needed to be killed.

Study design

The effect of MR activation during the development of obesity and related disorders was evaluated for its involvement in the transition towards HF. Animals of both genotypes ($SHHF^{cp/cp}$ and $SHHF^{+/+}$) were given the selective MRA eple (pure active molecule provided by *Pfizer*) from 1.5 months onwards (Figure 1A). This time point corresponds to the onset of metabolic disorders (dyslipidaemia, insulin resistance and overweight) and the pre-hypertensive stage in the absence of any apparent signs of cardiac dysfunction to date (Youcef *et al.*, 2014). Eple treatment was provided in drinking water at a final concentration of 100 $mg{\cdot}kg^{-1}{\cdot}day^{-1}$. The choice of this dosage was based on data from several reports (Lacolley *et al.*, 2002; Bayorh *et al.*, 2006; Rigsby *et al.*, 2007; Susic *et al.*, 2007; Baldo *et al.*, 2011; Fraccarollo *et al.*, 2011; Miana *et al.*, 2011; Watson *et al.*, 2013). Although much higher than that prescribed to patients with HF, the MRA concentration used herein is justified by the differences in drug metabolism and efficacy of the compounds between rats and humans. In order to minimize the effects of subjective bias when assessing results, each experimenter was blinded to the assignment of animals to the different treatment groups especially for echocardiography and haemodynamic evaluations.

In order to facilitate the description of the various experimental groups, the following nomenclature is used throughout the paper: the time (expressed in months) at which the observations/assays were performed is indicated as a number in front of the SHHF strain (for example, $^{1.5}$SHHF refers to observations made at 1.5 months of age); the genotype is indicated by a sign after SHHF (as $SHHF^{+/+}$ or $SHHF^{cp/cp}$), while the treatment status with eple is indicated with the suffix 'eple'. The absence of eple indicates that these rats are part of a control placebo group.

Ten $SHHF^{cp/cp}$ and 10 $SHHF^{+/+}$ rats were allocated to the $^{1.5}$SHHF group. From 1.5 to 12.5 months of age, the regular monitoring of the metabolic and cardiovascular parameters of the four experimental groups ($SHHF^{+/+}$eple, n = 8; $SHHF^{cp/cp}$eple, n = 11; $SHHF^{+/+}$, n = 10 and $SHHF^{cp/cp}$, n = 8) allowed the comparison of their respective phenotypes at different time points up to 11 months of follow-up (Figure 1a).

Echocardiography

Transthoracic echocardiographies were performed at 1.5, 3, 6, 9.5, 11.5 and 12.5 months of age on anesthetized rats (isoflurane, 5% at induction and 3% for maintenance, in 1.5 $L{\cdot}min^{-1}$ O_2) using a 12 MHz transducer (Sonos 5500 Ultrasound System, Philips) (Youcef *et al.*, 2014). Animals were positioned in left decubitus to acquire a short axis view of the left ventricle (LV) and an apical four-chamber view.

Morphological parameters of the LV were assessed using the two-dimensional (2D) M mode: LV internal diameter at the end diastole (LVIDd), at the end systole (LVIDs), posterior wall and septum thicknesses (PWT and SWT, respectively) were recorded to enable the calculation of LV mass according to the following equation, $LVmass = 1.04*[(PWT + SWT + LVIDd)^3 - (LVIDs)^3]$, where 1.04 is the estimated specific gravity of the myocardium.

LV systolic function was assessed by (i) 2D M mode to calculate the ejection fraction (EF) as follows: $EF\ (\%) = [(EDV - ESV)/EDV \times 100]$, where EDV and ESV correspond to the end-diastolic and end-systolic volumes respectively, and (ii) offline

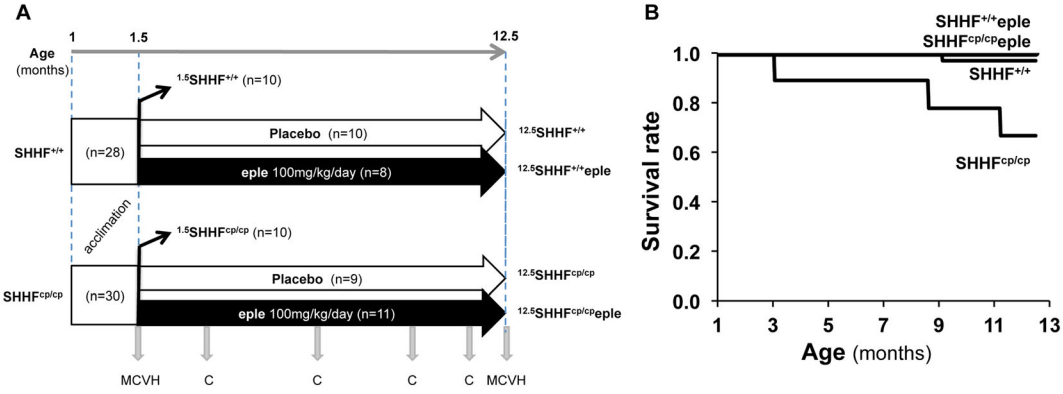

Figure 1

Study design and survival rate. (A) Thirty $SHHF^{cp/cp}$ and 28 $SHHF^{+/+}$rats were randomized either to the $^{1.5}$SHHF group (1.5-month follow-up, n = 10 per genotype) or to the long-term follow-up group to receive either the selective MRA eplerenone (eple 100 $mg{\cdot}kg^{-1}{\cdot}day^{-1}$) ($^{12.5}SHHF^{+/+}$eple, n = 8 and $^{12.5}SHHF^{cp/cp}$eple, n = 11) or placebo ($^{12.5}SHHF^{+/+}$, n = 10 and $^{12.5}SHHF^{cp/cp}$, n = 9). Animals underwent metabolic (M), cardiac (C), vascular (V) and histological (H) phenotyping at the beginning and at the end of the study. Cardiac parameters were regularly monitored from 1.5 to 12.5 months of age. (B) Kaplan–Meier curves indicating the survival rate for each studied group.

tissue Doppler imaging at the lateral and septal mitral annulus in the apical four-chamber view which assesses longitudinal LV function and measures Sa wave velocity.

LV diastolic function and LV filling pressures were assessed by pulse wave Doppler performed on the apical four-chamber view. This allowed the measurement and calculation of the ratio of the early (E) to late (A) ventricular filing waves, the isovolumetric relaxation time (IVRT), the E wave deceleration time (EDT), while the e′ mitral wave by tissue Doppler imaging allowed the evaluation of diastolic function of the myocardium. The LV filling pressures were determined by the E/e′ ratio. All echocardiographic examinations were based on the calculation of the mean of three consecutive cardiac cycles and were performed by a single experienced sonographer. The group sizes varied along the follow-up due to loss of animals in untreated groups and to the restricted access to the echocardiographic transducer.

Fasting glycaemia, blood biochemical and hormonal assays

Blood samples were drawn from the carotid artery of killed 16 h-fasted animals. Sera were obtained after a 20-min incubation period at room temperature and centrifugation at 1000x *g* for 15 min. Serum lipid profiles [total cholesterol, triglycerides (TG), high-density and low-density lipoproteins (HDL and LDL respectively) and free fatty acids] were assessed by an automatic biochemistry analyser using enzymatic methods. Sodium and potassium (Na^+, K^+) were measured by a standardized indirect potentiometry technique. Adiponectin and insulin levels were determined by ELISA (adiponectin Rat ELISA kit #ab108784 and insulin Human ELISA kit, #ab100578, respectively).

Insulin resistance (IR) was estimated by the HOMA-IR index:

$$\text{HOMA-IR} = [\text{fasting plasma glucose } (\text{mmol}\cdot\text{L}^{-1}) \times \text{fasting plasma insulin } (\mu\text{IU}\cdot\text{mL}^{-1})]/22.5.$$

Plasma samples were obtained by adding sodium citrate anticoagulant to a subset of the blood samples immediately followed by centrifugation at 1700x *g* for 10 min and subsequent retrieval of the supernatant. Circulating levels of brain natriuretic peptide (BNP) were measured by ELISA (BNP 45 Rat ELISA Kit #ab108816). Aldosterone and corticosterone levels were measured on 24-h urine samples with commercial kits according to the manufacturer's recommendations (Siemens 06615154 Coat-A-Count RIA Aldosterone Kit and AssayMax Corticosterone ELISA Kit, Assaypro, St. Charles, MO, USA, respectively). Fasting glycaemia was measured on a drop of venous blood from conscious rats using a glucometer (Freestyle Papillon Easy, Abbott).

Total RNA isolation and RT qPCR assays

Total RNAs were isolated from a transverse section of the myocardium including portions of both ventricles (RNA Now, Ozyme) and their purity and integrity verified by spectrophotometry and capillary electrophoresis (NanoDrop® ND-1000 spectrophotometer and Agilent 2100 Bioanalyzer with RNA 6000 Nano assay kit respectively). Only RNAs with no sign of high levels of DNA contamination or marked degradation (RNA Integrity Number > 8) were considered of good quality and used for further analysis.

Briefly, reverse transcriptions (RT) of 400 ng of total RNA into cDNA were performed using the Qiagen RT^2 First Strand Kit according to the manufacturer's protocol. Real-time quantitative PCR (qPCR) was subsequently performed with Qiagen Custom RT^2 Profiler PCR Arrays on 2.27 ng of cDNA per well using Qiagen RT^2 SYBR Green Mastermixes. Triplicate assays were run for each gene of interest [fibronectin 1 (fn1; vimentin (vim); tissue growth factor 2, tgb2; tissue growth factor 3 (tgb3); collagen 3a1 (col3a1); NADPH oxidase 4 (Nox4)] in the ViiA7 PCR system (Life Technologies) using the default settings. Comparative threshold cycles (C_T) data were used to calculate relative gene expression values, by applying the RT^2 Profiler PCR Array Data Analysis software v3.5, available online at http://pcrdataanalysis.sabiosciences.com/pcr/arrayanalysis.php. C_T for Sdha, Actb and B2m genes, considered as housekeeping genes, were used for qPCR data normalization. Fold changes in the gene expressions studied (Qiagen reference upon request) were calculated as $2^{(-\Delta CT)}$. Results are expressed as the ratio of $2^{(-\Delta CTSHHFeple)}/2^{(-\Delta CTSHHF)}$ for each transcript in each genotype studied. The *P*-values were calculated using Student,*s t*-test.

Histology

Immediately after the animals had been killed, $^{12.5}$SHHF right carotid, heart and perirenal visceral adipose tissue (VAT) were rapidly dissected, rinsed in saline solution (NaCl 0.9%) and formalin fixed for further histological analysis. Perirenal location was preferred over other locations because it was always present even in the $^{12.5}$SHHF$^{+/+}$ rats where very few small VAT pads developed. Serial 5-μm sections of paraffin embedded tissues were prepared for heart and carotid while 10-μm sections were prepared for VAT. Carotids were stained using the Weigert's orcein-fuchsin method to determine the medial cross-sectional area by manually delineating the carotid edges of several serial carotid slides for each rat using the NIS-element software (Nikon). Hearts and perirenal VAT were stained with Sirius red to determine the degree of myocardial fibrosis and distribution of cross-sectional adipocyte area (CSAA) respectively using ImageJ software. Myocardial fibrotic area was analysed by measuring the % of fibrotic area (demonstrated as magenta staining) of whole heart sections. CSAA was measured for each adipocyte representing the VAT sections from each rat.

Statistical analysis

The data and statistical analysis comply with the recommendations on experimental design and analysis in pharmacology (Curtis *et al.*, 2015). However, some limitations apply: randomization was not used for *in vivo* experiments as the littermate status (genetic link) of the purchased rats was not known, and the group sizes varied in the follow-up due to the restricted access to the echocardiographic transducer and biochemistry laboratory.

All analyses were performed using SAS R9.3 software (SAS Institute, Cary, NC, USA). The overall two-tailed significance level was set at $P < 0.05$. Two-way ANOVA with genotype (SHHF$^{+/+}$ vs. SHHF$^{cp/cp}$) and treatment (placebo vs. eple) along with their interaction as fixed effects were performed, followed by four *post hoc* pairwise comparisons of interest

(when the overall probability of the model was significant) effect of treatment according to genotype (placebo vs. eple for each genotype) and effect of genotype according to treatment ($SHHF^{+/+}$ vs. $SHHF^{cp/cp}$ in each treatment group). The significance level for comparisons was adjusted for multiplicity in order to preserve the overall 5% error rate using the formula $\alpha' = 1 - (1 - \alpha)^{1/k}$, where α and α′ are the overall and adjusted significance levels respectively, and k is the number of comparisons (four comparisons; $^*P < 0.05$). Results are presented for each parameter and each time point as global results (sample size, *P*-values of the model and the fixed effects), adjusted means and SEM (mean values adjusted for the effect of other factors) and the four pairwise comparisons of interest for which the significance level has to be set to $P < 0.0127$ in order to preserve the overall 5% α error rate. Of note, pairwise comparison results were only considered in the cases of significant interaction ($P < 0.05$).

Statistical analysis of the CSAA measured in adipose tissue sections was performed using a Mann–Whitney test to compare the difference between $^{12.5}SHHF^{cp/cp}$ and $^{12.5}SHHF^{cp/cp}$ eple rats ($^*P < 0.05$). All results are expressed as adjusted means ± SEM.

To evaluate how variations in metabolic parameters may be associated with cardiac phenotypes, a statistical analysis of the raw data obtained from each group of animals were combined and computed in the COExpress software (Nazarov *et al.*, 2013). Pearson's test was conducted to calculate the correlation coefficients (*r*) and a *P*-value <0.05 was considered to identify the significant parameters that may associate together. Correlation coefficients rank from +1 to −1, where +1 means a strict positive correlation and −1 denotes a strict negative correlation.

Results

The present study design allowed the evaluation of the preventive effects of long-term eple treatment observed in the presence of metabolic disorders in obese $SHHF^{cp/cp}$ rats and to compare these effects with those observed in lean $SHHF^{+/+}$ rats (Figure 1A). Preventive effects were expected given that eple treatment was started before any cardiac symptoms were observed (1.5 months of age) in control lean $SHHF^{+/+}$ rats. The end point of the study (month 12.5) was chosen so as to maintain the number of surviving untreated $SHHF^{cp/cp}$ rats to an appropriate level to allow statistical comparison with the other groups of rats (Figure 1B). The effective delivery of eple was confirmed by the measurement of urinary excretions of aldosterone and corticosterone, which were significantly increased and decreased respectively, upon treatment in both genotypes (Supporting Information Table S1).

Haemodynamic and vascular parameters are not affected by eplerenone monotherapy

Mean blood pressure and pulse pressure calculations were based on the invasive measurement of central blood pressures (diastolic blood pressure and systolic blood pressure) of anaesthetized $^{12.5}SHHFeple$ and their genotype-matched untreated controls. The results demonstrated the presence of severe hypertension whose severity was independent of both genotype and of MRA treatment (Supporting Information Table S2). The distensibility-pressure curve as well as analysis of compliance, elastic incremental modulus (Einc) and wall stress values demonstrated that the intrinsic mechanical behaviour of the carotid wall was similar across all groups at 12.5 months of age (Supporting Information Table S2 and Fig. S1A and B). The lack of effect of eple on SBP (systolic blood pressure) was confirmed on conscious animals during plethysmographic evaluation of their peripheral blood pressure (Supporting Information Table S3).

Metabolic disorders accelerate adverse cardiac remodelling in $SHHF^{cp/cp}$ rats compared with $SHHF^{+/+}$ controls

Echocardiographic follow-up between 1.5 and 12.5 months of age revealed that $SHHF^{+/+}$-untreated rats developed LV concentric hypertrophic remodelling as evidenced by the stability of the LVIDd values (Figure 2A) and the diastolic

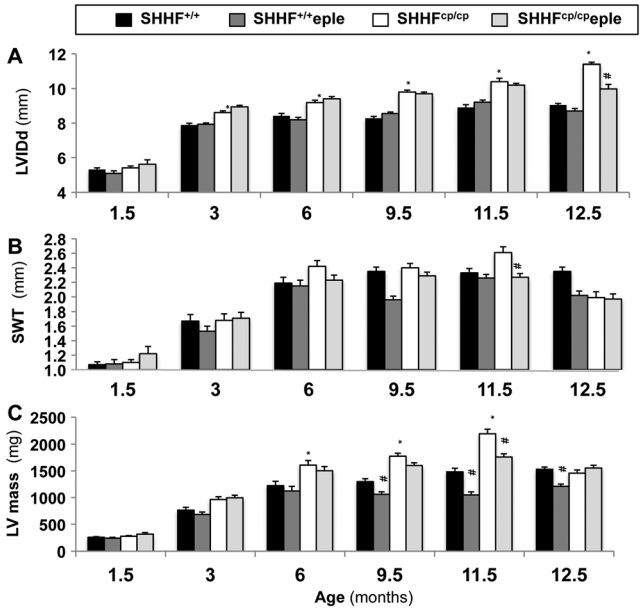

Figure 2

Chronic eple treatment alleviates cardiac remodelling. Cardiac remodelling of $SHHF^{+/+}$ (black), $SHHF^{+/+}$eple (dark grey), $SHHF^{cp/cp}$ (white) and $SHHF^{cp/cp}$eple (light grey) rats was evaluated by echocardiographic follow-up. At 1.5 months of age $n = 9$, $SHHF^{+/+}$ rats were evaluated then $n = 8$ of them at the other time points; $n = 8$ $SHHF^{+/+}$eple were evaluated at each time point; $n = 8$ $SHHF^{cp/cp}$ were evaluated at 1.5, 3 and 6 months, $n = 7$ of them at 9 months and $n = 6$ of them at 11.5 and 12.5 time points. Finally, $n = 10$ $SHHF^{cp/cp}$eple were evaluated from 1.5 to 11. 5 months of age and n = 11 of them at 12.5 months allowing the determination of (A) left ventricular internal diameter at end diastole (LVIDd), (B) septum wall thickness (SWT) and (C) calculation of left ventricular mass (LV mass). Two-way ANOVA with genotype ($SHHF^{+/+}$ vs. $SHHF^{cp/cp}$) and treatment (placebo vs. eple) was performed, and the significance level was set to $P < 0.0127$. $^*P < 0.0127$ for the comparison between the genotypes at the same age, $\#P < 0.0127$ for the comparison of the untreated and treated animals from the same genotype at the same age.

thickening of the septal wall (SWT) (Figure 2B) resulting in an increased LV mass (Figure 2C).

When compared with the lean rats, SHHF$^{cp/cp}$ animals exhibited worsened phenotypes. Only 60% of untreated SHHF$^{cp/cp}$ rats survived until 12.5 months of age, while 90% of SHHF$^{+/+}$ rats completed the protocol (Figure 1B). This observation was explained in part by sudden cardiac death due to the development of end-stage systolic dysfunction observed with ageing in this genotype. Compared with SHHF$^{+/+}$ rats, $^{11.5}$SHHF$^{cp/cp}$ rats developed LV eccentric remodelling characterized by a decrease in SWT and an increase in both LVIDd and LVmass (Figure 2A–C). In addition, in $^{12.5}$SHHF$^{cp/cp}$ LV dilation was exacerbated (Figure 2A), while SWT (Figure 2B) decreased. LV remodelling was accompanied by a greater interstitial fibrosis in $^{12.5}$SHHF$^{cp/cp}$ rats than in $^{12.5}$SHHF$^{+/+}$ rats (Figure 3A and B).

From 1.5 to 11.5 months of age, SHHF$^{cp/cp}$ rats exhibited a progressive alteration of their diastolic function (increased IVRT and EDT values over time, Figure 4A and B). By 12.5 months, SHHF$^{cp/cp}$ LV remodelling was exacerbated by concomitant functional alterations. $^{12.5}$SHHF$^{cp/cp}$ rats exhibited altered diastolic function and increased filling pressures (reduced IVRT and EDT values, Figure 4A and B) as well as a decline in systolic function (reduced EF values, Figure 4D) compared with $^{12.5}$SHHF$^{+/+}$ rats. The reduction in Sa (marker of an altered longitudinal shortening and lengthening of the myocardium) observed in $^{12.5}$SHHF$^{cp/cp}$ rats further characterized the decline in their systolic function ($^{12.5}$SHHF$^{cp/cp}$ Sa = 2.64 ± 0.10 cm·s^{-1} vs. $^{12.5}$SHHF$^{+/+}$ Sa = 3.41 ± 0.07 cm·s^{-1}; Figure 4C).

The accelerated decline in cardiac function in SHHF$^{cp/cp}$ rats in comparison with SHHF$^{+/+}$ rats arose in part from the early onset of drastic metabolic disorders. Already overweight at 1.5 months of age ($^{1.5}$SHHF$^{cp/cp}$ = 150 ± 4 g vs. $^{1.5}$SHHF$^{+/+}$ = 133 ± 2 g; Figure 5A), $^{1.5}$SHHF$^{cp/cp}$ rats exhibited dyslipidaemia that dramatically and significantly worsened with ageing when compared with SHHF$^{+/+}$ rats (Table 1). While the genotype did not influence fasting glycaemia, $^{12.5}$SHHF$^{cp/cp}$ insulin and adiponectin levels were increased by approximately fourfold and decreased by approximately twofold, respectively, when compared with $^{12.5}$SHHF$^{+/+}$ animals (Table 1). This paralleled the development of massive visceral obesity in SHHF$^{cp/cp}$ rats [body weight (BW), ^{12}SHHF$^{cp/cp}$BW = 787 ± 17 g vs. ^{12}SHHF$^{+/}$

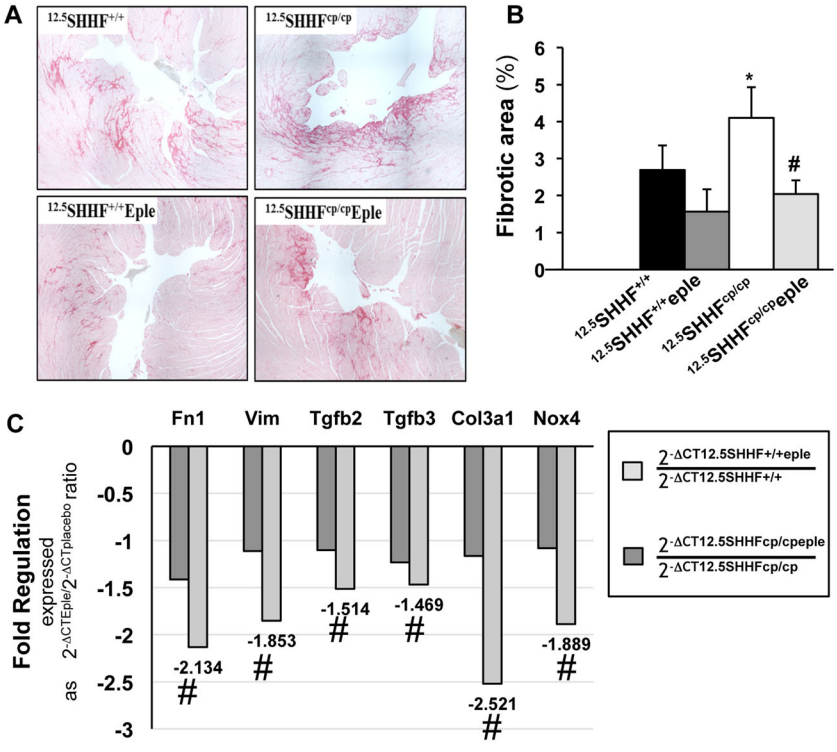

Figure 3

Chronic eple treatment reduces myocardial fibrosis. Myocardial fibrosis and the anti-fibrotic effects of eple were measured at the histological and molecular levels on rat myocardium. (A) Sections of paraffin-embedded hearts obtained from untreated (upper panels) and MRA-treated (lower panels) $^{12.5}$SHHF$^{+/+}$ and $^{12.5}$SHHF$^{cp/cp}$ animals ($^{12.5}$SHHF$^{+/+}$, n = 5; $^{12.5}$SHHF$^{+/+}$eple, n = 6; $^{12.5}$SHHF$^{cp/cp}$, n = 4; $^{12.5}$SHHF$^{cp/cp}$eple, n = 6) were stained with Sirius red enabling the identification of fibrotic areas (evidenced in magenta). (B) Fibrotic areas in each experimental group were quantified using ImageJ software and expressed as percentage of total section area. (C) The impact of eple on mRNA expression levels of genes involved in cardiac fibrosis and remodelling [fibronectin (Fn1), vimentin (Vim), transforming growth factor β2 and β3 (Tgfb2 and Tgfb3), collagen 3 type α 1 (Col3a1) and NADPH oxidase 4 (Nox4)] was assessed in cardiac tissue from $^{12.5}$SHHF$^{+/+}$eple rats compared with $^{12.5}$SHHF$^{+/+}$ rats (light grey, n = 4) and in $^{12.5}$SHHF$^{cp/cp}$eple rats compared with $^{12.5}$SHHF$^{cp/cp}$ rats by RT-qPCR (dark grey, n = 4). Comparative threshold cycles (C_T) for Sdha, Actb and B2m genes, considered as housekeeping genes, were used for qPCR data normalization. Gene fold regulation is expressed as the ratio of ΔCT of the treated group over the ΔCT of the placebo group of the same genotype at 12.5 months of age. #$P < 0.05$ for the comparison of the untreated and treated animals from the same genotype at the same age by Student's t-test.

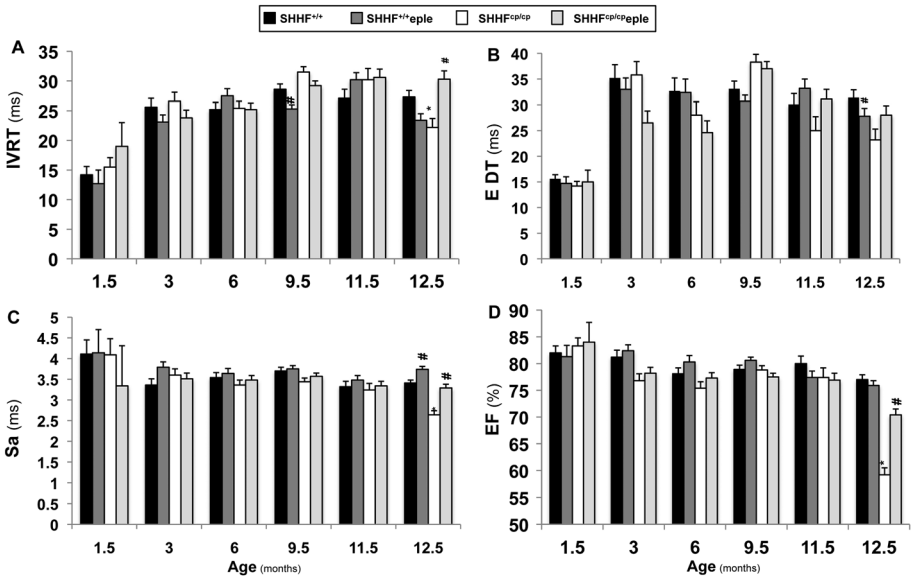

Figure 4

Chronic eple treatment improves SHHF$^{cp/cp}$ cardiac functional parameters. Echocardiographic monitoring of cardiac functional parameters where at 1.5 months of age $n = 9$ SHHF$^{+/+}$ rats were evaluated then $n = 8$ of them at the other time points; $n = 8$ SHHF$^{+/+}$eple were evaluated at each time point; $n = 8$ SHHF$^{cp/cp}$ were evaluated at 1.5, 3 and 6 months, $n = 7$ of them at 9 months and $n = 6$ of them at 11.5 and 12.5 time points. Finally, $n = 10$ SHHF$^{cp/cp}$eple were evaluated from 1.5 to 11. 5 months of age and $n = 11$ of them at 12.5 months. (A) Isovolumic relaxation time (IVRT), (B) E wave deceleration time (EDT), (C) Sa duration (Sa) and (D) ejection fraction (EF). Two-way ANOVA with genotype (SHHF$^{+/+}$ vs. SHHF$^{cp/cp}$) and treatment (placebo vs. eple) was performed, and the significance level was set to $P < 0.0127$. *$P < 0.0127$ for the comparison between the genotypes at the same age, #$P < 0.0127$ for the comparison of the untreated and treated animals from the same genotype at the same age.

$^{+}$BW = 456 ± 14 g] (Figure 5A). Characterization of $^{12.5}$SHHF$^{cp/cp}$ perirenal adipocyte size (mean cross-sectional area) and distribution (median) (inserts within Figure 5B panels) revealed significantly larger adipocyte size and broader distribution than that observed in $^{12.5}$SHHF$^{+/+}$ rats (Figure 5B left panels).

Altogether, the above results indicate that the presence of metabolic disorders in SHHF$^{cp/cp}$ rats are associated with adverse cardiac remodelling in these obese rats as compared with lean SHHF$^{+/+}$ rats, resulting in an impairment of $^{12.5}$SHHF$^{cp/cp}$ diastolic and systolic functions.

Preventive chronic eplerenone monotherapy mainly preserves SHHF$^{cp/cp}$ myocardial structure and function

Preventive effects of eplerenone in SHHF$^{+/+}$eple rats. Initiation of the 11-month eple treatment at 1.5 months of age in lean SHHF$^{+/+}$ rats had preventive effects on their cardiac phenotypes. Chronic MRA treatment significantly and sustainably reduced the hypertrophic remodelling by preventing SW thickening as early as 9.5 months of age (Figure 2B). Although myocardial fibrosis was detectable in $^{12.5}$SHHF$^{+/+}$ rats (Figure 3A, upper left panel), its quantification (Figure 3B) did not reveal any significant effect of eple treatment. Molecular characterization (Figure 3C) of myocardial fibrosis was also assessed by the relative quantification of several transcripts encoding for structural and extracellular matrix proteins [fibronectin (Fn1), vimentin (Vim), transforming growth factor 2 and 3 (Tgfb2 and Tgfb3 respectively), collagen type 3a1 (Col3a1) and NADPH oxidase 4 (Nox4)]. None of these transcripts exhibited a significant reduction in their expression levels. The assessment of SHHF$^{+/+}$ diastolic (IVRT and EDT) and systolic (Sa and EF) cardiac function also demonstrated fairly stable parameters with ageing, none of which were significantly affected by eple treatment (Figure 4 A–D, black and dark grey columns).

Hence, the prevention of LV concentric remodelling observed in lean SHHF$^{+/+}$eple rats suggests that they modestly but significantly benefited from the early initiation of eple treatment.

Greater benefits of eplerenone treatment in obese SHHF$^{cp/cp}$ rats

Chronic MRA alleviated the cardiac eccentric remodelling of SHHF$^{cp/cp}$eple rats by significantly reducing their LV mass at 11.5 months of age (Figure 2C) and heart weight/tibia length ratio at age 12.5 months ($^{12.5}$SHHF$^{cp/cp}$eple HW/TL = 49.5 ± 1.3 mg·mm^{-1} vs. $^{12.5}$SHHF$^{cp/cp}$ HW/TL = 57 ± 1.7 mg·mm^{-1}). Eple treatment also prevented the LV remodelling of $^{12.5}$SHHF$^{cp/cp}$eple myocardium by limiting its dilation and septal thickening (Figure 2A and B). These structural improvements in $^{12.5}$SHHF$^{cp/cp}$eple LV were accompanied by a significant reduction in myocardial fibrosis, initially evaluated and quantified at the histological level (Figure 3A and B, #$P < 0.05$) and subsequently confirmed at the molecular level using RT-qPCR (Figure 3C). Significant down-regulations of Fn1, Vim, Tgfb2, Tgfb3, Col3a1 and Nox4 were demonstrated upon treatment in the $^{12.5}$SHHF$^{cp/cp}$eple myocardium when compared with their $^{12.5}$SHHF$^{cp/cp}$ untreated controls (Figure 3C).

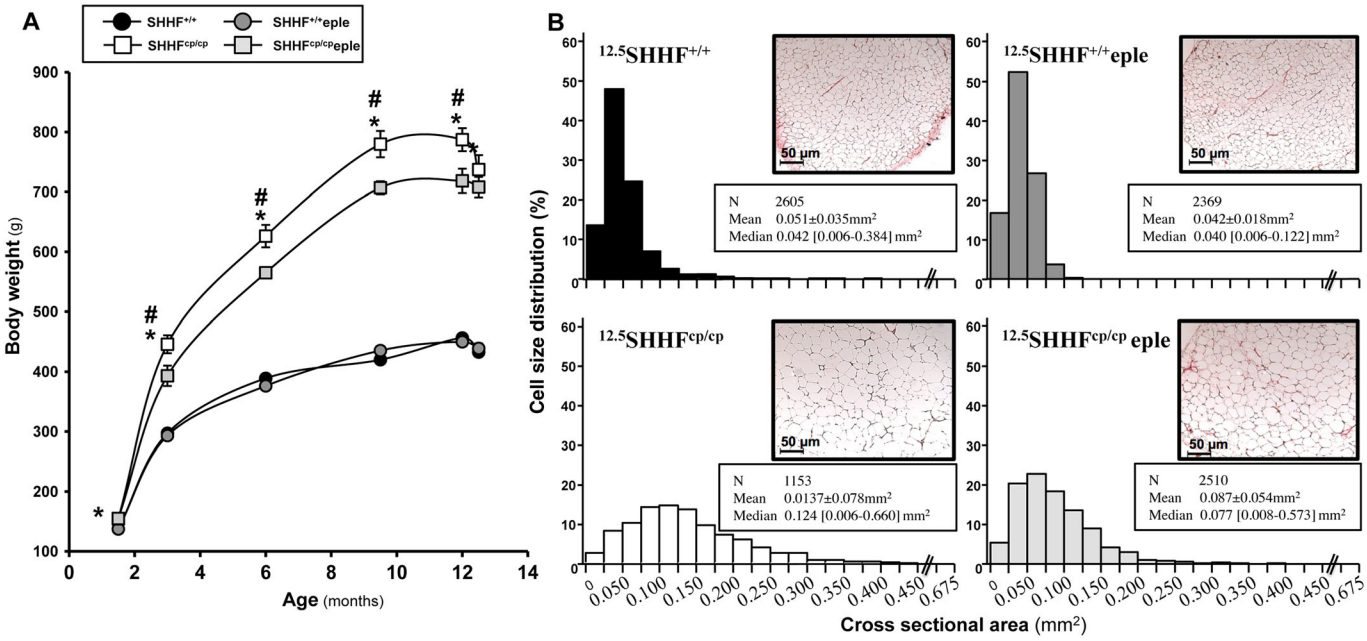

Figure 5

Chronic eple treatment reduces body weight gain and visceral adipocyte hypertrophy. Rats received either MRA (eple, 100 mg·kg^{-1}·day^{-1}) or placebo from the age of 1.5 months up to 12.5 months. (A) Follow-up of animal body weight (BW). At 1.5 months of age $n = 9$, SHHF$^{+/+}$ rats were evaluated then $n = 8$ of them at the other time points; $n = 8$ SHHF$^{+/+}$eple were evaluated at each time point; $n = 8$ SHHF$^{cp/cp}$ were evaluated at 1.5, 3 and 6 months, $n = 7$ of them at 9 months and $n = 6$ of them at 11.5 and 12.5 time points. Finally, $n = 11$ SHHF$^{cp/cp}$eple were evaluated at each time point. *$P < 0.05$ SHHF$^{cp/cp}$ compared with SHHF$^{+/+}$ at the same age; #$P < 0.05$ treated group compared with the untreated group of the same genotype at the same age by Student's *t*-test. (B) Morphological analysis of perirenal VAT dissected at month 12.5. Analysis of VAT sections stained with Sirius red allowing the measurement of the cross-sectional adipocyte area (CSAA, mm^2) and cell size distribution (%) of the adipocyte population from each experimental group (SHHF$^{+/+}$ $n = 5$; SHHF$^{+/+}$eple $n = 4$; SHHF$^{cp/cp}$ $n = 5$; SHHF$^{cp/cp}$ eple $n = 8$).

At 12.5 months of age, chronic eple treatment had no significant effect on myocardial MR transcript expression in either genotype (not shown) but significantly decreased the expression of the Hsd11β1 transcript (encoding for the enzyme converting cortisone into corticosterone) only in $^{12.5}$SHHF$^{cp/cp}$eple rats (Hsd11β1 transcript $2^{-\Delta CT12.5SHHFcp/cpeple}/2^{-\Delta CT12.5SHHFcp/cp} = -1.466$).

At 12.5 months of age, chronic eple treatment had no significant effect on perirenal adipose tissue Hsd11β1 transcript expression in either genotype (not shown). This did not exclude the possible participation of this enzyme to the observed VAT phenotypes at earlier time points than the end of the study, but suggested that the effects on phenotype were mostly as a result of MR antagonism in adipose tissue.

Diastolic function preservation

In HF pathophysiology, the link between structure and function is relatively straightforward in particular for diastolic function, which is adversely affected by LV hypertrophy. In addition to the reduction in cardiac hypertrophy, results relative to cardiac functional parameters (Figure 4A–D) showed that eple prevented the myocardial relaxation impairment already observed in ^{3}SHHF$^{cp/cp}$ rats. At the age of 3 months, diastolic parameters were less altered in the eple group, as demonstrated by a significant increase in EDT upon treatment (^{3}SHHF$^{cp/cp}$eple EDT = 26.5 ± 2.3 ms vs. ^{3}SHHF$^{cp/cp}$ EDT = 35.8 ± 2.6 ms) and a concomitant trend for a smaller E wave velocity ((^{3}SHHF$^{cp/cp}$eple E = 114 mm·s^{-1} vs. ^{3}SHHF$^{cp/cp}$ E = 106 mm·s^{-1}). In the $^{12.5}$SHHF$^{cp/cp}$eple group, treatment also prevented the increase in E/A (not shown) and the decrease in IVRT (Figure 4A).

Systolic function preservation

Eple further improved cardiac systolic function in the $^{12.5}$SHHF$^{cp/cp}$eple group by preventing the drop in Sa wave observed in $^{12.5}$SHHF$^{cp/cp}$ controls ($^{12.5}$SHHF$^{cp/cp}$eple Sa = 3.29 ± 0.09 cm·s^{-1} vs. $^{12.5}$SHHF$^{cp/cp}$ Sa = 2.64 ± 0.10 cm·s^{-1}, $P < 0.0001$) as well as the decrease in EF (Figure 4C and D). Concomitant with the observed alteration in systolic function in obese placebo $^{12.5}$SHHF$^{cp/cp}$ rats, an increase in LV filling pressure was also noted, as shown not only by the decrease in IVRT and EDT (Figure 4A and B) but also by an elevation in E/e′ and E/A ratios, which were prevented by eple treatment (not shown).

Altogether, these results demonstrate that SHHF$^{cp/cp}$eple animals greatly benefited from early eple treatment by reducing the adverse cardiac remodelling observed in their untreated controls. The treatment positively affected both diastolic as well as systolic functions and delayed the onset of HF in the obese rats by preserving the decline in LV function.

Chronic eplerenone further benefits obese SHHF$^{cp/cp}$ rats by greatly improving their metabolic status

While long-term MR antagonism had no effect on SHHF$^{+/+}$eple body weight (BW), eple significantly and sustainably

Table 1

Mineralocorticoid receptor blockade reduces dyslipidemia and preserves adiponectinemia

Experimental group *n*	$^{1.5}$SHHF$^{+/+}$ *7*	$^{12.5}$SHHF$^{+/+}$ *10*	$^{12.5}$SHHF$^{+/+}$eple *8*	$^{1.5}$SHHF$^{cp/cp}$ *7*	$^{12.5}$SHHF$^{cp/cp}$ *6*	$^{12.5}$SHHF$^{cp/cp}$eple *11*	ANOVA Genotype	ANOVA Treatment	ANOVA Interaction
Lipid profile, g·L^{-1}	0.69 ± 0.03	0.90 ± 0.25	0.75 ± 0.28	0.93 ± 0.03	4.25 ± 0.33*	2.67 ± 0.24$^{\#}$	<0.05	<0.05	<0.05
Total chol.									
HDL	0.24 ± 0.01	0.25 ± 0.02	0.27 ± 0.02	0.30 ± 0.01	0.56 ± 0.02*	0.50 ± 0.02	<0.05	NS	NS
LDL	0.38 ± 0.03	0.08 ± 0.00	0.08 ± 0.01	0.48 ± 0.03	1.48 ± 0.40*	0.55 ± 0.08$^{\#}$	<0.05	<0.05	<0.05
TG	0.37 ± 0.01	0.61 ± 2.02	0.58 ± 2.26	0.77 ± 0.14	20.5 ± 2.6*	8.26 ± 1.93$^{\#}$	<0.05	<0.05	<0.05
FFA	1.2 ± 0.1	0.4 ± 0.0	0.3 ± 0.1	1.6 ± 0.2	1.0 ± 0.2	1.5 ± 0.3	<0.05	NS	NS
Fasting glycemia, mmol·L^{-1}	4.6 ± 0.4	5.7 ± 0.4	6.1 ± 0.4	5.7 ± 0.5	5.4 ± 0.6	6.4 ± 0.4	NS	NS	NS
Fasting insulin, μIU·mL^{-1}	11 ± 2	12 ± 5	10 ± 5	16 ± 4	52 ± 6*	69 ± 5	<0.05	NS	NS
HOMA-IR index	0.8 ± 0.2	0.9 ± 0.5	0.9 ± 0.5	2.6 ± 0.8	3.6 ± 0.6*	5.4 ± 0.6	<0.05	NS	NS
Ionogram, mmol·L^{-1} Na^{+}	141 ± 0	143 ± 3	139 ± 3	140 ± 1	146 ± 3	140 ± 2	NS	NS	NS
K^{+}	4.8 ± 0.2	4.9 ± 0.2	5.2 ± 0.2	4.9 ± 0.1	4.6 ± 0.3	5.0 ± 0.2	NS	NS	NS
Na^{+}/K^{+} ratio	29.9 ± 1.4	30.2 ± 1.9	27.1 ± 2.0	28.9 ± 0.6	33.1 ± 2.3	28.4 ± 1.7	NS	NS	NS
Adiponectin, μg·mL^{-1}	6.3 ± 0.4	6.3 ± 1.3	7.4 ± 1.2	19.7 ± 1.4	11.9 ± 0.7*	22.7 ± 1.6$^{\#}$	<0.05	<0.05	<0.05
BNP, pg·mL^{-1}	135 ± 18	219 ± 25	208 ± 25	102 ± 15	225 ± 29	203 ± 22	NS	NS	NS

HDL, high-density lipoprotein; LDL, low-density lipoprotein; FFA, free fatty acids; TG, triglyceride; Na^{+}, sodium, K^{+}, potassium; BNP, brain natriuretic peptide. Values are the mean ± SEM. Two-factor non-parametric ANOVAs analysis with two factors allowed the evaluation of interaction between genotype and treatment at 12.5 months of age. Pairwise comparison for adjusted multiple testing set to $P < 0.0127$ in order to preserve the 5% overall α error rate.

*To compare SHHF cp/cp versus SHHF+/+ at the same time point.

$^{\#}$To compare eple versus placebo for a same genotype; NS, non-significant; *n* represents for the number of samples.

reduced SHHF$^{cp/cp}$eple BW reaching a maximal value at 12-months of age (^{12}SHHF$^{cp/cp}$epleBW = 718 ± 13 g vs. ^{12}SHHF$^{cp/cp}$BW = 787 ± 17 g) (Figure 5A). Eple treatment significantly minimized weight gain of ^{12}SHHF$^{cp/cp}$-treated rats (563 ± 43 g gained) when compared with ^{12}SHHF$^{cp/cp}$-untreated rats (634 ± 27 g gained) and this was achieved without significantly modifying their food and water intake or their 24 h urinary excretion (data not shown). Eple had no impact on the size and distribution of $^{12.5}$SHHF$^{+/+}$ adipocytes (Figure 5B, upper panels) although chronic MRA treatment resulted in significantly less hypertrophy of $^{12.5}$SHHF$^{cp/cp}$eple adipocytes than that observed in untreated controls (Figure 5 B, lower panels).

Eple monotherapy partially prevented the respective increases in total cholesterol (−40%), LDL (−65%) and TG (−60%) concentrations as well as the decrease in adiponectin blood concentration observed in $^{12.5}$SHHF$^{cp/cp}$ controls (Table 1). MRA treatment had no significant effects on either the Na^+/K^+ ratio, excluding any potential toxic effect on salt and water balance due to the long-term use of the MRA (Table 1), or on BNP plasma levels in surviving animals at the end of the study.

Thus, SHHF$^{cp/cp}$eple rats benefited from eple treatment at both the cardiac and metabolic level. Together, these phenotypic improvements participated in a greater survival rate as indicated by the Kaplan–Meier representation where 100% of SHHF$^{cp/cp}$eple rats completed the protocol (Figure 1B).

Correlation of metabolic and cardiac physiological profiles of all experimental groups

The statistical correlations of several metabolic and cardiac physiological parameters of the six experimental groups ($^{1.5}$SHHF$^{+/+}$; $^{1.5}$SHHF$^{cp/cp}$; $^{12.5}$SHHF$^{+/+}$; $^{12.5}$SHHF$^{+/+}$eple; $^{12.5}$SHHF$^{cp/cp}$ and $^{12.5}$SHHF$^{cp/cp}$eple) are presented as a correlogram in Figure 6. This approach allowed a better understanding of the evolution of selected cardiac parameters (vertical columns) using the probability of a significant relationship with metabolic values independently of the age, the genotype and the treatment (horizontal lines). Correlation coefficients (*r*) are systematically ranked between −1 to +1, where −1 value represents a perfect negative correlation between two variables, while + 1 represents a perfect positive correlation. The darker blue and red squares indicate a significant strong positive (from 0.6 to 1) and negative (from −1 to −0.6) correlation, respectively, while squares in light blue and pink denote a significant intermediate correlation (from 0.2 to 0.6 and from −0.6 to −0.2 respectively). The grey squares show the non-significant-matched parameters.

In the present series, regardless of the genotype, the age and the treatment, the high values of the metabolic parameters (Ins, LDL, HDL, Tot Chol and TG serum levels) were systematically and significantly correlated with high heart weight (HW) values and their lower values were statistically correlated with lower HW values. Together, these above-cited parameters exhibit a statistically positive correlation between each other (blue squares). Conversely, Ins, LDL, HDL, total cholesterol and TG serum levels showed a very systematic and significant negative correlation (red squares) with the cardiac ejection fraction (EF), suggesting that when those metabolic parameters rise, the systolic function is depressed.

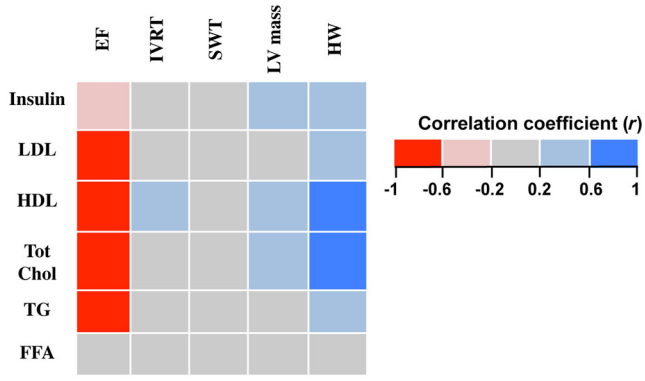

Figure 6

Correlation of metabolic and cardiac physiological profiles of all experimental groups. The CoExpress software was used for calculating correlation coefficients (r) based on Pearson's test between physiological parameters and the corrplot function to elaborate the depicted correlogram. Grey coloured rectangles are poorly correlated and not significant (pVal > 0.05) while the coloured scale bar ranges from red (*r* from −1 to −0.6) to dark blue (*r* from 0.6 to 1) and intermediate values (*ar* from −0.6 to −0.2 in pink and from 0.2 to 0.6 in light blue). Cardiac parameters are represented horizontally with EF denoting ejection fraction; IVRT, isovolumetric relaxation time; SWT, septum wall thickness; LV mass, left ventricle mass; HW, heart weight. Metabolic parameters are represented vertically with LDL, HDL denoting low-density and high-density lipoprotein respectively; Tot Chol, total cholesterol; TG, triglycerides and FFA, free fatty acids.

Discussion and conclusion

The efficacy of eple in preventing the obesity-accelerated progression towards HF was assessed in the present study over a course of the longest treatment duration reported to date in the literature. The design of the present study allowed us to demonstrate long-term sustained effects of eple and their modulation by the presence (SHHF$^{cp/cp}$) or absence (SHHF$^{+/+}$) of metabolic disorders. Using this specific approach, we demonstrated that chronic MR antagonism initiated when young pre-hypertensive SHHF rats are at risk of developing HF but not yet symptomatic was able to sustainably prevent cardiac remodelling in a haemodynamically-independent manner. Incremental benefits were further observed when the preventive treatment was given to pre-hypertensive, overweight and dyslipidaemic SHHF$^{cp/cp}$ rats. Indeed and as suggested by the correlation data, eple had the most striking effects on traits related to obesity by reducing weight gain, adipocyte hypertrophy and dyslipidaemia, all of which contributed to the prevention of cardiac remodelling and alterations in function in SHHF$^{cp/cp}$eple rats. While clinical data are limited regarding the ability of MRA to prevent the risk of developing HF in obese patients, our results strongly suggest that in the context of obesity, the targeted antagonism of MR overactivation appears as a promising therapeutic approach in this setting. Our study provides evidence that will potentially open new avenues for drug repositioning of MRA for the prevention of HF, particularly in high-risk patients presenting obesity-related disorders.

Compared with other studies (Rocha *et al.*, 1998; Bender *et al.*, 2013; Cezar *et al.*, 2013), our data further characterized the anti-fibrotic properties of eple in the context of obesity by

assessing the sustained long-term effects of this MRA. The decrease in Tgfb2 (mostly expressed in epithelial cells) and Tgfb3 (primarily expressed in mesenchymal cells), Col3a1, Fn 1, Nox4 and Vim transcripts upon eple treatment strongly suggests that MR activation is also involved in the deleterious differentiation of cardiac fibroblasts into myofibroblasts. Such differentiation is known to occur during HF development (Cucoranu *et al.*, 2005; Heymans *et al.*, 2015) and during the endothelial-to-mesenchymal transition that is reactivated in the diseased adult heart (Welch-Reardon *et al.*, 2015). The reduced expression of the Nox4 transcript in $^{12.5}$SHHF$^{cp/cp}$eple rats also suggests that the beneficial effect of MRA is partly the result of sustained anti-oxidative stress effects previously reported shortly after the initiation of the treatment (Kuster *et al.*, 2005; Bender *et al.*, 2015).

The eple-induced down-regulation of these transcripts furthermore alleviated the alterations in cardiac diastolic relaxation, LV stiffness, hypertrophy and subsequent dilated remodelling observed in SHHF$^{cp/cp}$eple rats, thus confirming preclinical data obtained when MRA treatment was given for a shorter duration (Rocha *et al.*, 1998; Cezar *et al.*, 2013; Bender *et al.*, 2015). The unique therapeutic opportunity provided by early preventive MRA administration enabled the SHHF$^{cp/cp}$eple rats to be protected from developing diastolic dysfunction as the increase in filling pressures and early impairment of myocardial relaxation were prevented. While the sudden death of the sickest animals in the control SHHF$^{cp/cp}$-untreated group prevented the detection of significant differences in systolic function prior to the last echocardiographic time point, eple treatment nonetheless significantly preserved the systolic function of these SHHF$^{cp/cp}$eple rats. Furthermore, given that the severity of myocardial fibrosis has been associated with long-term mortality in HF patients (Azevedo *et al.*, 2010; Aoki *et al.*, 2011; Fraccarollo *et al.*, 2011), it is likely that myocardial fibrosis caused the lower survival rate observed in untreated animals, while the anti-fibrotic property of eple contributed to the improved survival rate of the SHHF$^{cp/cp}$ eple rats.

Given the pleiotropic activity of the MR, it is likely that the observed beneficial effects may also be related to MR antagonism in other MR target organs in addition to the myocardium and adipose tissues. Because metabolic disorders are well-established risk factors for developing cardiovascular diseases, the authors cannot refute the possibility that the prevention of hepatocellular damage mediated by MRA treatment, demonstrated in non-alcoholic fatty liver disease experimental models by others (Wada *et al.*, 2010, 2013; Pizarro *et al.*, 2015), is also involved in the global improvement of the health of treated rats. Of interest, the efficacy of eple at ameliorating histological steatosis and hepatic fibrosis in mice even allows us to consider the MR as a novel potential therapeutic target for insulin resistance and non-alcoholic liver diseases (Pizarro *et al.*, 2015). Likewise, an improvement in kidney function (Kang *et al.*, 2009; Lian *et al.*, 2012) as well as decreased sympathetic drive and improved baroreflex functions in HF are likely to contribute to the reported beneficial effects of MRA treatment. In addition to this pleiotropic effect of MR, the down-regulation of the Hsd11b1 enzyme in the myocardium upon MRA treatment might also participate in the cardiac phenotype improvement by locally reducing the inflammatory response. Further analyses are required to better comprehend certain discrepancies in the reported metabolic effects of MRA that are difficult to reconcile or inconsistent with previous results reported in the literature, as outlined in Supporting Information Table S4 (Bender *et al.*, 2015; Bostick *et al.*, 2015). Antihypertensive and glucose homeostasis properties of the MRA could have been masked by the complexity of the SHHF strain and/or the 11-month duration of the treatment, highlighting long-term chronic effects rather than an acute response to MRA, as mostly described in the literature. In the SHHF strain, the development of metabolic and hypertensive disorders is genetically determined rather than diet-induced (such as in high-fat/high-fructose and high-salt diets), and several concomitant neuroendocrine alterations (Heyen *et al.*, 2002; Radin *et al.*, 2003; Radin *et al.*, 2008; Przybylski *et al.*, 2010) have been reported in addition to hyperaldosteronism. Moreover, MRAs vary in their effects and some of the differences reported between the effects of spironolactone and eple may result from the fact that eple is devoid of the anti-progesterone, anti-androgenic and anti-glucogenic side effects of spironolactone. Notwithstanding the latter, the eple-induced overall protection reported in the present study is predominantly the result of MR antagonism because eple is only marginally antagonistic to other receptors. The absence of expected insulin-sensitivity properties of the preserved levels of circulating adiponectin could be explained by the fact that one of the adiponectin target organs, the liver, was shown to develop severe non-alcoholic steatosis in the SHHF$^{cp/cp}$ rat (Youcef *et al.*, 2014) that may preclude its favourable response to adiponectin. Of note, such impairments in the benefits of adiponectin have previously been reported in obese experimental models (Hui *et al.*, 2012). Likewise, the absence of BNP regulation upon treatment is likely to be a reflection of the complex relationship between the amount of visceral fat distribution and BNP levels (Clerico *et al.*, 2012).

While the above issues remain to be investigated in the SHHF model and in tissues other than the myocardium and visceral adipocyte pads, eple treatment had conversely striking effects on preventing the development of dyslipidaemia and the decrease in adiponectin concentration in $^{12.5}$SHHF$^{cp/cp}$eple rats, both of which are considered to be good prognostic factors in HF patients. The fact that adiponectin is reported to act directly on cardiomyocytes, alleviating the development of hypertrophy, cardiomyopathy and systolic dysfunction (Goldstein *et al.*, 2009), is also consistent with its participation in the preservation of cardiac function in the present model (Guo *et al.*, 2008; Hirata *et al.*, 2009; Armani *et al.*, 2014).

There is also accumulating evidence suggesting that MR overactivation mediates pathophysiological changes that participate in the development of MetS and the associated decline in cardiovascular function. Clinical reports support the notion that hypertensive and primary hyperaldosteronism patients exhibit more frequent impairment of metabolic signalling, dyslipidaemia and obesity (Manrique *et al.*, 2005; Van Gaal *et al.*, 2006; Sowers, 2007). Corticosterone is an upstream precursor molecule of the mineralocorticoid aldo. Upon eple treatment, the myocardial transcript of the enzyme responsible for its production, Hsd11β1and its urinary levels were decreased. This suggests that eple treatment interrupted the positive feedback loop in which MR activation participates in the up-regulation of Hsd11β1 gene

expression (Nagata *et al.*, 2006). Because aldo is synthesized from an upper precursor, that is, cholesterol, one could also speculate that a similar positive feedback loop is also present between MR activation and regulation of cholesterol levels, which may explain the anti-cholesterol effect of MRA treatment in our experimental model. To the best of our knowledge, the effect of MRA on dyslipidaemia in humans has only been described in the ASCOT clinical trial where MRA treatment reduced hyperlipidaemia (reduction in total and LDL cholesterol levels) in individuals with resistant hypertension (Chapman *et al.*, 2007). This purported MRA effect on dyslipidaemia could potentially benefit from *post hoc* analyses of data collected in large trials evaluating the effect of MRA on HF patients in order to reinforce the data obtained in the small pilot trials by Kosmala *et al.* (2012, 2013). In agreement with *in vitro* as well as the sparse *in vivo* findings, our results indicate that MR activation is involved as a crucial regulator of adipocyte function and hypertrophy (Caprio *et al.*, 2007; Hirata *et al.*, 2009; Wada *et al.*, 2013). More importantly, our findings further demonstrate that the reported reduced adipocyte hypertrophy observed after shorter treatment durations *in vivo* (Caprio *et al.*, 2007; Hirata *et al.*, 2009) was sustained after 11 months and may account in part for the rarely described reduced weight gain previously observed in ^{3}SHHF$^{cp/cp}$eple rats. The fact that the BW of SHHF$^{+/+}$eple rats was not affected by eple treatment indicates that it has very minor effect, if any, on lean body mass.

Obesity and its associated metabolic abnormalities are major risk factors for the development of HF (Rimbaud *et al.*, 2009; Lai *et al.*, 2014). The correlogram of metabolic parameters with the cardiac parameters clearly demonstrate the physiological association between metabolic and cardiac parameters in our experimental model. The increased metabolic values paralleled the increases in cardiac remodelling and diastolic dysfunction (correlation of LV mass and HW with metabolic parameters), while the increased metabolic values paralleled the decrease in systolic function (negative correlation of EF with metabolic parameters). Our results further demonstrated that MRA not only delayed LV remodelling and dysfunction but also improved dyslipidaemia. Together with the improvement in adipocyte hypertrophy in SHHF$^{cp/cp}$ rats, eple was found to have a beneficial effect on lipid homeostasis, which most likely contributed to preserving the quality of cardiac energy sources and the delay in HF development. Eple thus appears to be a promising drug that could prevent ventricular remodelling and cardiac function by preserving cardiac energy metabolism.

Given that late eple administration either rarely (Bender *et al.*, 2015) or mostly fails to reverse cardiac outcomes (Susic *et al.*, 2007; Cezar *et al.*, 2013), the use of eple as a preventive rather than curative drug should be considered and further investigated in HF with preserved EF. Such an early treatment approach was assessed clinically in the treatment of HF with preserved EF using the MRA spironolactone (Pfeffer *et al.*, 2015) but overall only neutral results were obtained. A *post hoc* analysis of the regional variation of this study concluded that the patients from America were the only patients benefiting from spironolactone treatment (Pfeffer *et al.*, 2015). However, the baseline characteristics of these American patients displayed higher body mass index (32.9 vs. 29.4 kg·m^{-2}) and dyslipidaemia (71 vs. 49%) than their Russian/Georgian counterparts. In the present experimental model, SHHF$^{cp/cp}$ and SHHF$^{+/+}$ closely mimicked these patient group differences at baseline, and, likewise, our findings revealed a greater benefit of MRA in the metabolically-affected subgroups of rats.

In summary, the present findings demonstrate that long-term chronic MRA treatment started before the onset of cardiac alterations was beneficial to both lean and obese SHHF rats and contributed in delaying progression to the development of HF symptoms. These latter rats further benefited from the treatment through an improvement in their metabolic parameters. Given the converging evidence of the major role of excessive MR activation as an independent risk factor for metabolic and subsequent cardiovascular disease, our results support the use of MRA as a promising therapeutic strategy for the prevention of cardiac diseases especially in HF patients with altered metabolic parameters.

Acknowledgements

We are thankful to Clément L'Huillier, Arnaud Bianchi and Anne-Laure Leblanc for their expert technical assistance in histology and animal handling. The authors thank Pierre Pothier for the critical reading of the manuscript. This work was funded by Institut National de la Santé et de la Recherche Médicale (Inserm), Région Lorraine, Fondation pour la Recherche Médicale (FRM) comité Lorrain, FP7 FIBRO-TARGETS grant agreement no: 602904. G. Youcef received a salary grant from the Fonds National pour la Recherche (FNR) Luxembourg. We are grateful to Pfizer Inc. (New York, NY) for providing part of the eplerenone.

Author contributions

G.Y., A.O., N.N., A.M., C.D., R.M.R.G., C.L. and A.P. performed the research. A.P., F.Z. and L.V. designed the research study. R.M.R.G., C.L., R.F. and A.M. contributed essential tools. A.P., G.Y., A.O., C.L., R.F., F.Z. and P.L. analysed the data. A.P., G.Y., A.O., F.J., F.Z., P.L. and L.V. wrote the paper.

Conflict of interest

The authors disclose no conflicts of interest.

Declaration of transparency and scientific rigour

This Declaration acknowledges that this paper adheres to the principles for transparent reporting and scientific rigour of preclinical research recommended by funding agencies, publishers and other organizations engaged with supporting research.

References

Alexander SP, Cidlowski JA, Kelly E, Marrion N, Peters JA, Benson HE *et al.* (2015a). The Concise Guide to PHARMACOLOGY 2015/16: Nuclear hormone receptors. Br J Pharmacol 172: 5956–5978.

Alexander SP, Fabbro D, Kelly E, Marrion N, Peters JA, Benson HE *et al.* (2015b). The Concise Guide to PHARMACOLOGY 2015/16: Catalytic receptors. Br J Pharmacol 172: 5979–6023.

Aoki T, Fukumoto Y, Sugimura K, Oikawa M, Satoh K, Nakano M *et al.* (2011). Prognostic impact of myocardial interstitial fibrosis in non-ischemic heart failure. -Comparison between preserved and reduced ejection fraction heart failure. Circ J 75: 2605–2613.

Armani A, Cinti F, Marzolla V, Morgan J, Cranston GA, Antelmi A *et al.* (2014). Mineralocorticoid receptor antagonism induces browning of white adipose tissue through impairment of autophagy and prevents adipocyte dysfunction in high-fat-diet-fed mice. FASEB J 28: 3745–3757.

Azevedo CF, Nigri M, Higuchi ML, Pomerantzeff PM, Spina GS, Sampaio RO *et al.* (2010). Prognostic significance of myocardial fibrosis quantification by histopathology and magnetic resonance imaging in patients with severe aortic valve disease. J Am Coll Cardiol 56: 278–287.

Baldo MP, Forechi L, Morra EA, Zaniqueli D, Machado RC, Lunz W *et al.* (2011). Long-term use of low-dose spironolactone in spontaneously hypertensive rats: effects on left ventricular hypertrophy and stiffness. Pharmacol Rep 63: 975–982.

Bayorh MA, Mann G, Walton M, Eatman D (2006). Effects of enalapril, tempol, and eplerenone on salt-induced hypertension in dahl salt-sensitive rats. Clin Exp Hypertens 28: 121–132.

Bender SB, McGraw AP, Jaffe IZ, Sowers JR (2013). Mineralocorticoid receptor-mediated vascular insulin resistance: an early contributor to diabetes-related vascular disease? Diabetes 62: 313–319.

Bender SB, DeMarco VG, Padilla J, Jenkins NT, Habibi J, Garro M *et al.* (2015). Mineralocorticoid receptor antagonism treats obesity-associated cardiac diastolic dysfunction. Hypertension 65: 1082–1088.

Bostick B, Habibi J, DeMarco VG, Jia G, Domeier TL, Lambert MD *et al.* (2015). Mineralocorticoid receptor blockade prevents Western diet-induced diastolic dysfunction in female mice. Am J Physiol Heart Circ Physiol 308: H1126–H1135.

Caprio M, Feve B, Claes A, Viengchareun S, Lombes M, Zennaro MC (2007). Pivotal role of the mineralocorticoid receptor in corticosteroid-induced adipogenesis. FASEB J 21: 2185–2194.

Caprio M, Antelmi A, Chetrite G, Muscat A, Mammi C, Marzolla V *et al.* (2011). Antiadipogenic effects of the mineralocorticoid receptor antagonist drospirenone: potential implications for the treatment of metabolic syndrome. Endocrinology 152: 113–125.

Cezar MD, Damatto RL, Martinez PF, Lima AR, Campos DH, Rosa CM *et al.* (2013). Aldosterone blockade reduces mortality without changing cardiac remodelling in spontaneously hypertensive rats. Cell Physiol Biochem 32: 1275–1287.

Chapman N, Dobson J, Wilson S, Dahlof B, Sever PS, Wedel H *et al.* (2007). Effect of spironolactone on blood pressure in subjects with resistant hypertension. Hypertension 49: 839–845.

Clark AL, Fonarow GC, Horwich TB (2014). Obesity and the obesity paradox in heart failure. Prog Cardiovasc Dis 56: 409–414.

Clerico A, Giannoni A, Vittorini S, Emdin M (2012). The paradox of low BNP levels in obesity. Heart Fail Rev 17: 81–96.

Cucoranu I, Clempus R, Dikalova A, Phelan PJ, Ariyan S, Dikalov S *et al.* (2005). NAD(P)H oxidase 4 mediates transforming growth factor-beta1-induced differentiation of cardiac fibroblasts into myofibroblasts. Circ Res 97: 900–907.

Curtis MJ, Bond RA, Spina D, Ahluwalia A, Alexander SP, Giembycz MA *et al.* (2015). Experimental design and analysis and their reporting: new guidance for publication in BJP. Br J Pharmacol 172: 3461–3471.

De Keulenaer GW, Brutsaert DL (2011). Are systolic and diastolic heart failure overlapping or distinct phenotypes within the heart failure spectrum? Circulation 123: 1996–2005.

Feraco A, Armani A, Mammi C, Fabbri A, Rosano GM, Caprio M (2013). Role of mineralocorticoid receptor and renin-angiotensin-aldosterone system in adipocyte dysfunction and obesity. J Steroid Biochem Mol Biol 137: 99–106.

Fraccarollo D, Berger S, Galuppo P, Kneitz S, Hein L, Schutz G *et al.* (2011). Deletion of cardiomyocyte mineralocorticoid receptor ameliorates adverse remodelling after myocardial infarction. Circulation 123: 400–408.

Goldstein BJ, Scalia RG, Ma XL (2009). Protective vascular and myocardial effects of adiponectin. Nat Clin Pract Cardiovasc Med 6: 27–35.

Greenberg B, Zannad F, Pitt B (2006). Role of aldosterone blockade for treatment of heart failure and post-acute myocardial infarction. Am J Cardiol 97: 34F–40F.

Guo C, Ricchiuti V, Lian BQ, Yao TM, Coutinho P, Romero JR *et al.* (2008). Mineralocorticoid receptor blockade reverses obesity-related changes in expression of adiponectin, peroxisome proliferator-activated receptor-gamma, and proinflammatory adipokines. Circulation 117: 2253–2261.

Heyen JR, Blasi ER, Nikula K, Rocha R, Daust HA, Frierdich G *et al.* (2002). Structural, functional, and molecular characterization of the SHHF model of heart failure. Am J Physiol Heart Circ Physiol 283: H1775–H1784.

Heymans S, Gonzalez A, Pizard A, Papageorgiou AP, Lopez-Andres N, Jaisser F *et al.* (2015). Searching for new mechanisms of myocardial fibrosis with diagnostic and/or therapeutic potential. Eur J Heart Fail 17: 764–771.

Hirata A, Maeda N, Hiuge A, Hibuse T, Fujita K, Okada T *et al.* (2009). Blockade of mineralocorticoid receptor reverses adipocyte dysfunction and insulin resistance in obese mice. Cardiovasc Res 84: 164–172.

Homma T, Fujisawa M, Arai K, Ishii M, Sada T, Ikeda M (2012). Spironolactone, but not eplerenone, impairs glucose tolerance in a rat model of metabolic syndrome. J Vet Med Sci 74: 1015–1022.

Hui X, Lam KS, Vanhoutte PM, Xu A (2012). Adiponectin and cardiovascular health: an update. Br J Pharmacol 165: 574–590.

Iraqi W, Rossignol P, Angioi M, Fay R, Nuee J, Ketelslegers JM *et al.* (2009). Extracellular cardiac matrix biomarkers in patients with acute myocardial infarction complicated by left ventricular dysfunction and heart failure: insights from the Eplerenone Post-Acute Myocardial Infarction Heart Failure Efficacy and Survival Study (EPHESUS) study. Circulation 119: 2471–2479.

Ishizuka T, Ernsberger P, Liu S, Bedol D, Lehman TM, Koletsky RJ *et al.* (1998). Phenotypic consequences of a nonsense mutation in the leptin receptor gene (fak) in obese spontaneously hypertensive Koletsky rats (SHROB). J Nutr 128: 2299–2306.

Kang YS, Ko GJ, Lee MH, Song HK, Han SY, Han KH *et al.* (2009). Effect of eplerenone, enalapril and their combination treatment on diabetic nephropathy in type II diabetic rats. Nephrol Dial Transplant 24: 73–84.

Kilkenny C, Browne W, Cuthill IC, Emerson M, Altman DG (2010). NC3Rs Reporting Guidelines Working Group. Br J Pharmacol 160: 1577–1579.

Kosmala W, Jedrzejuk D, Derzhko R, Przewlocka-Kosmala M, Mysiak A, Bednarek-Tupikowska G (2012). Left ventricular function impairment in patients with normal-weight obesity: contribution of abdominal fat deposition, profibrotic state, reduced insulin sensitivity, and proinflammatory activation. Circ Cardiovasc Imaging 5: 349–356.

Kosmala W, Przewlocka-Kosmala M, Szczepanik-Osadnik H, Mysiak A, Marwick TH (2013). Fibrosis and cardiac function in obesity: a randomised controlled trial of aldosterone blockade. Heart 99: 320–326.

Kuster GM, Kotlyar E, Rude MK, Siwik DA, Liao R, Colucci WS *et al.* (2005). Mineralocorticoid receptor inhibition ameliorates the transition to myocardial failure and decreases oxidative stress and inflammation in mice with chronic pressure overload. Circulation 111: 420–427.

Lacolley P, Labat C, Pujol A, Delcayre C, Benetos A, Safar M (2002). Increased carotid wall elastic modulus and fibronectin in aldosterone-salt-treated rats: effects of eplerenone. Circulation 106: 2848–2853.

Lai YH, Liu CC, Kuo JY, Hung TC, Wu YJ, Yeh HI *et al.* (2014). Independent effects of body fat and inflammatory markers on ventricular geometry, midwall function, and atrial remodeling. Clin Cardiol 37: 172–177.

Lian M, Hewitson TD, Wigg B, Samuel CS, Chow F, Becker GJ (2012). Long-term mineralocorticoid receptor blockade ameliorates progression of experimental diabetic renal disease. Nephrol Dial Transplant 27: 906–912.

Manrique J, Diaz A, Gavira JJ, Hernandez A, Pujante D, Errasti P (2005). Preliminary results of the effect of treatment of hyperhomocysteinemia and its relationship with inflammation, coagulation status, and endothelial function after renal transplantation. Transplant Proc 37: 3782–3784.

Marzolla V, Armani A, Zennaro MC, Cinti F, Mammi C, Fabbri A *et al.* (2012). The role of the mineralocorticoid receptor in adipocyte biology and fat metabolism. Mol Cell Endocrinol 350: 281–288.

McGrath JC, Lilley E (2015). Implementing guidelines on reporting research using animals (ARRIVE etc.): new requirements for publication in BJP. Br J Pharmacol 172: 3189–3193.

McMurray JJ, Petrie MC, Murdoch DR, Davie AP (1998). Clinical epidemiology of heart failure: public and private health burden. Eur Heart J 19 (Suppl P): P9–16.

Miana M, de Las Heras N, Rodriguez C, Sanz-Rosa D, Martin-Fernandez B, Mezzano S *et al.* (2011). Effect of eplerenone on hypertension-associated renal damage in rats: potential role of peroxisome proliferator activated receptor gamma (PPAR-gamma). J Physiol Pharmacol 62: 87–94.

Nagata K, Obata K, Xu J, Ichihara S, Noda A, Kimata H *et al.* (2006). Mineralocorticoid Receptor Antagonism Attenuates Cardiac Hypertrophy and Failure in Low-Aldosterone Hypertensive Rats. Hypertension 47: 656–664.

Nazarov PV, Reinsbach SE, Muller A, Nicot N, Philippidou D, Vallar L *et al.* (2013). Interplay of microRNAs, transcription factors and target genes: linking dynamic expression changes to function. Nucleic Acids Res 41: 2817–2831.

Pawson AJ, Sharman JL, Benson HE, Faccenda E, Alexander SP, Buneman OP *et al.* (2014). The IUPHAR/BPS guide to PHARMACOLOGY: an expert-driven knowledge base of drug targets and their ligands. Nucleic Acids Res 42: D1098–D1106.

Pfeffer MA, Claggett B, Assmann SF, Boineau R, Anand IS, Clausell N *et al.* (2015). Regional variation in patients and outcomes in the Treatment of Preserved Cardiac Function Heart Failure With an Aldosterone Antagonist (TOPCAT) trial. Circulation 131: 34–42.

Pizarro M, Solis N, Quintero P, Barrera F, Cabrera D, Rojas-de Santiago P *et al.* (2015). Beneficial effects of mineralocorticoid receptor blockade in experimental non-alcoholic steatohepatitis. Liver Int 35: 2129–2138.

Przybylski R, McCune S, Hollis B, Simpson RU (2010). Vitamin D deficiency in the spontaneously hypertensive heart failure [SHHF] prone rat. Nutr Metab Cardiovasc Dis 20: 641–646.

Radin MJ, Holycross BJ, Hoepf TM, McCune SA (2003). Increased salt sensitivity secondary to leptin resistance in SHHF rats is mediated by endothelin. Mol Cell Biochem 242: 57–63.

Radin MJ, Holycross BJ, Hoepf TM, McCune SA (2008). Salt-induced cardiac hypertrophy is independent of blood pressure and endothelin in obese, heart failure-prone SHHF rats. Clin Exp Hypertens 30: 541–552.

Ramirez E, Klett-Mingo M, Ares-Carrasco S, Picatoste B, Ferrarini A, Ruperez FJ *et al.* (2013). Eplerenone attenuated cardiac steatosis, apoptosis and diastolic dysfunction in experimental type-II diabetes. Cardiovasc Diabetol 12: 172.

Rigsby CS, Pollock DM, Dorrance AM (2007). Spironolactone improves structure and increases tone in the cerebral vasculature of male spontaneously hypertensive stroke-prone rats. Microvasc Res 73: 198–205.

Rimbaud S, Garnier A, Ventura-Clapier R (2009). Mitochondrial biogenesis in cardiac pathophysiology. Pharmacol Rep 61: 131–138.

Rocha R, Chander PN, Khanna K, Zuckerman A, Stier CT Jr (1998). Mineralocorticoid blockade reduces vascular injury in stroke-prone hypertensive rats. Hypertension 31: 451–458.

Sowers JR (2007). Metabolic risk factors and renal disease. Kidney Int 71: 719–720.

Susic D, Varagic J, Ahn J, Matavelli L, Frohlich ED (2007). Long-term mineralocorticoid receptor blockade reduces fibrosis and improves cardiac performance and coronary hemodynamics in elderly SHR. Am J Physiol Heart Circ Physiol 292: H175–H179.

van Deursen VM, Damman K, van der Meer P, Wijkstra PJ, Luijckx GJ, van Beek A *et al.* (2014). Co-morbidities in heart failure. Heart Fail Rev 19: 163–172.

Van Gaal LF, Mertens IL, De Block CE (2006). Mechanisms linking obesity with cardiovascular disease. Nature 444: 875–880.

Wada T, Kenmochi H, Miyashita Y, Sasaki M, Ojima M, Sasahara M *et al.* (2010). Spironolactone improves glucose and lipid metabolism by ameliorating hepatic steatosis and inflammation and suppressing enhanced gluconeogenesis induced by high-fat and high-fructose diet. Endocrinology 151: 2040–2049.

Wada T, Miyashita Y, Sasaki M, Aruga Y, Nakamura Y, Ishii Y *et al.* (2013). Eplerenone ameliorates the phenotypes of metabolic syndrome with NASH in liver-specific SREBP-1c Tg mice fed high-fat and high-fructose diet. Am J Physiol Endocrinol Metab 305: E1415–E1425.

Watson LE, Jewell C, Song J, Dostal DE (2013). Echocardiographic effects of eplerenone and aldosterone in hypertensive rats. Front Biosci (Elite Ed) 5: 922–927.

Welch-Reardon KM, Wu N, Hughes CC (2015). A role for partial endothelial-mesenchymal transitions in angiogenesis? Arterioscler Thromb Vasc Biol 35: 303–308.

Youcef G, Olivier A, L'Huillier CP, Labat C, Fay R, Tabcheh L *et al.* (2014). Simultaneous characterization of metabolic, cardiac, vascular and renal phenotypes of lean and obese SHHF rats. PLoS One 9: e96452.

Zennaro MC, Caprio M, Feve B (2009). Mineralocorticoid receptors in the metabolic syndrome. Trends Endocrinol Metab 20: 444–451.

Supporting Information

Additional Supporting Information may be found in the online version of this article at the publisher's web-site:

http://dx.doi.org/10.1111/bph.13479

Figure S1 Carotid hemodynamic assessment.

Table S1 Influence of the eplerenone treatment on urinary aldosterone and corticosterone excretion.
Table S2 Lack of impact of eplerenone treatment on carotic hemodynamic properties.
Table S3 Chronic eplerenone treatment does not impact hemodynamic parameters in SHHF rats.
Table S4 Influence of eplerenone treatment applied as monotherapy in murine models.